Monthly Notices of the ROYAL ASTRONOMICAL SOCIETY

MNRAS **516,** 6172–6179 (2022) https://doi.org/10.1093/mnras/stac2622
Advance Access publication 2022 September 19

Oscillation modes and gravitational waves from strangeon stars

Hong-Bo Li [1,2] Yong Gao [1,2★] Lijing Shao [2,3★] Ren-Xin Xu [1,2★] and Rui Xu [2]

[1] *Department of Astronomy, School of Physics, Peking University, Beijing 100871, China*
[2] *Kavli Institute for Astronomy and Astrophysics, Peking University, Beijing 100871, China*
[3] *National Astronomical Observatories, Chinese Academy of Sciences, Beijing 100012, China*

Accepted 2022 September 12. Received 2022 August 10; in original form 2022 June 19

ABSTRACT

The strong interaction at low-energy scales determines the equation of state (EOS) of supranuclear matters in neutron stars (NSs). It is conjectured that the bulk dense matter may be composed of strangeons, which are quark clusters with nearly equal numbers of *u*, *d*, and *s* quarks. To characterize the strong-repulsive interaction at short distance and the non-relativistic nature of strangeons, a phenomenological Lennard–Jones model with two parameters is used to describe the EOS of strangeon stars (SSs). For the first time, we investigate the oscillation modes of non-rotating SSs and obtain their frequencies for various parametrizations of the EOS. We find that the properties of radial oscillations of SSs are different from those of NSs, especially for stars with relatively low central energy densities. Moreover, we calculate the f-mode frequency of non-radial oscillations of SSs within the relativistic Cowling approximation. The frequencies of the f mode of SSs are found to be in the range 6.7–8.7 kHz. Finally, we study the universal relations between the f-mode frequency and global properties of SSs, such as the compactness and the tidal deformability. The results we obtained are relevant to pulsar timing and gravitational waves, and will help to probe NSs' EOSs and infer non-perturbative behaviours in quantum chromodynamics.

Key words: asteroseismology – gravitational waves – stars: oscillations – pulsars: general.

1 INTRODUCTION

The equation of state (EOS) of nuclear dense matter plays a crucial role in many astrophysical phenomena associated with neutron stars (NSs; Lattimer & Prakash 2007; Ozel, Baym & Guver 2010; Abbott et al. 2018). Owing to the non-perturbative properties of the strong interaction at low energy, the EOS of dense matters at several nuclear densities still remains unknown. Witten (1984) conjectured that the true ground state of the dense matter is quark matter composed of almost free *u*, *d*, and *s* quarks. The pulsar-like compact objects should be quark stars (QSs) rather than conventional NSs. The MIT bag model with almost free quarks (Alcock, Farhi & Olinto 1986) and the colour-superconductivity state model (Alford et al. 2008) have been used in literature to study QSs. In 2003, Xu (2003) proposed that the constituting units of the supranuclear matter could be strange quark clusters, since the non-perturbative strong interaction may render quarks grouped in clusters. Each quark cluster is composed of several quarks (including *u*, *d*, and *s* flavours) condensing in position space rather than in momentum space. A name 'strangeon' is coined to these strange 'nucleons' (Lai & Xu 2017; Xu & Guo 2017). In this sense, compressed baryonic matter could be in a state of strangeons, and pulsar-like compact stars could thus be strangeon stars (SSs).

Strangeon matter, similar to strange quark matter, is composed of nearly equal numbers of *u*, *d*, and *s* quarks. However, different from strange quark matter, quarks in strangeon matter are localized inside strangeons due to the strong coupling between quarks. There are differences and similarities among NSs, QSs, and SSs. On the one hand, quarks are thought to be localized in strangeons in SSs, like neutrons in NSs. On the other hand, a strangeon, with light-flavour symmetry restoration of quark, may contain more than three valence quarks. In addition, the matter at the surface of SSs is strangeon matter, i.e. SSs are self-bound by the strong force, like QSs (Xu 2003). These properties are fundamental to a few important astrophysical observables. A sophisticated study on various global parameters of rotating SSs, including mass, radius, moment of inertia, tidal deformability, quadrupole moments, and shape parameters, was carried out by Gao et al. (2022).

SSs can account for many current observational facts in astrophysics. The EOS of SSs could be very stiff to explain the observed massive pulsars (Demorest et al. 2010; Antoniadis et al. 2013). The magnetospheric activity of SSs was discussed in Xu, Qiao & Zhang (1999). Lu et al. (2019) explained the sub-pulse drifting of radio pulsars using the properties at the surface of SSs. Also, pulsar glitches could be the result of star quakes (Peng & Xu 2008; Zhou et al. 2004, 2014), and a detailed modelling of the glitch behaviours confronted with observations was discussed in Lai et al. (2018b). The model of SSs can be extended to explain the glitch activity of normal radio pulsars (Wang et al. 2020). Recent studies (Lai et al. 2018a, 2021; Lai, Zhou & Xu 2019) have investigated the tidal deformability as well as the ejecta and light curve of merging binary SSs, showing consistency with the observations of the gravitational wave (GW) event GW170817 (Abbott et al. 2017) and its multiwavelength electromagnetic counterparts (Kasen et al. 2017; Kasliwal et al. 2017).

Owing to the difficulties in determining the EOS of pulsar-like compact stars from first principles, observations from different channels become important avenues in studying the EOS at high density, which can in turn be used to constrain microscopic laws (Ozel

★ E-mail: gaoyong.physics@pku.edu.cn (YG); lshao@pku.edu.cn (LS); r.x.xu@pku.edu.cn (R-XX)

et al. 2010). In this respect, GW asteroseismology that deals with oscillation modes offers a promising channel in the new era of GWs (Andersson & Kokkotas 1998; Benhar, Ferrari & Gualtieri 2004; Doneva et al. 2013; Andersson 2019). It is the focus of this study.

Radial oscillations of stellar models were studied in the pioneering works of Chandrasekhar (1964a,b). Notably, the properties of radial oscillations can give information about the stability and the EOS of compact stars. The first exhaustive compilation of radial oscillations for different zero-temperature EOSs was presented by Glass & Lindblom (1983). In Vaeth & Chanmugam (1992), the properties of radial modes of QSs were investigated. Furthermore, the study of radial oscillations of zero-temperature NSs can be extended to proto-NSs (Gondek, Haensel & Zdunik 1997). Because the EOS of proto-NSs is significantly softer than that of zero-temperature NSs, their spectra of the radial oscillation modes are very different. It is worth noting that Kokkotas & Ruoff (2001) presented a useful survey on the radial oscillation modes of NSs for various EOSs. Based on the equations presented by Misner, Thorne & Wheeler (1973), they showed that the derivatives in the linear differential equation can be written in the form of a self-adjoint differential operator. In this work, we calculate the frequencies of the first three radial modes of SSs using the method of the self-adjoint differential operator (Kokkotas & Ruoff 2001). By that we can investigate the properties of radial oscillations of SSs in detail and study the stability of SSs rigorously.

Non-radial oscillations of relativistic stars were studied in the pioneering work of Thorne & Campolattaro (1967). The oscillation modes are damped out due to the emission of GWs, so these oscillation modes are called quasi-normal modes (QNMs). For typical non-rotating relativistic fluid stars, QNMs are classified in polar and axial categories. The polar modes include the fundamental (f), pressure (p), and gravity (g) modes. The axial modes only have the space–time (w) modes, which are directly associated with the space–time metric and have no analogy in the Newtonian theory of stellar pulsations (Kokkotas & Schutz 1992). A detailed discussion about the relativistic perturbation equations was given in many works (see e.g. Lindblom & Detweiler 1983; Detweiler & Lindblom 1985; Chandrasekhar & Ferrari 1991; Allen et al. 1998; Kokkotas & Schmidt 1999). Using the Cowling approximation (Cowling 1941), Sotani et al. (2011) calculated non-radial oscillations of NSs with hadron–quark mixed phase transition. Besides, Doneva & Yazadjiev (2012) investigated non-radial oscillations of anisotropic NSs with polytropic EOSs. In Das et al. (2021), the impact of the dark matter on the f mode was also studied.

The f mode of NSs, QSs, and SSs is important for several reasons: (i) it depends on the EOS of compact stars; (ii) it is expected to be excited in many astrophysical scenarios and leads to efficient GW emission; (iii) its frequency is lower than other QNMs such as that of the p modes and the w modes, hence the f-mode oscillation is most likely to be detectable with a third-generation detector like the Einstein Telescope and the Cosmic Explorer (Punturo et al. 2010; Sathyaprakash et al. 2019; Kalogera et al. 2021), or even in an optimal case by the current generation LIGO/Virgo/KAGRA detectors (Abbott et al. 2019b, 2022; Abe et al. 2022). In this work, we calculate the f-mode frequency of SSs in the Cowling approximation and compare the results with those of NSs and QSs.

GW observation will be a powerful tool to study the EOS of compact stars in particular in the case that we have good empirical formulas for the QNMs as functions of stellar parameters. Indeed, universal empirical formulas relating the dynamical responses of a compact star under external perturbations – such as the f-mode frequency, the tidal and rotational deformations – to its global physical parameters – such as the mass, the radius, and the moment of inertia – have been discovered for NSs and QSs. For example, the I–Love–Q relations, discovered by Yagi & Yunes (2013a,b), relate the moment of inertia I, the tidal deformability λ, and the spin induced quadrupole moment Q. Another example is the relation for the f-mode frequency, the moment of inertia, and the tidal deformability (see e.g. Chan et al. 2014). Sotani & Kumar (2021) have investigated various universal relations between several oscillation modes and the tidal deformability. Inspired by works on the universal relations for single NSs (Andersson & Kokkotas 1998; Benhar et al. 2004; Doneva et al. 2013; Yagi & Yunes 2013a,b), recent studies have investigated various universal relations between the binary tidal deformability and the f-mode frequency of the post-merger remnant of a binary NS system using numerical relativity simulations (Bernuzzi, Dietrich & Nagar 2015b; Rezzolla & Takami 2016; Kiuchi et al. 2020). It is worth noting that Krüger & Kokkotas (2020b) and Manoharan, Krüger & Kokkotas (2021) calculated the f-mode frequency for fast-rotating NSs without using the Cowling approximation, and discovered a relation between the pre-merger tidal deformability and the dominant oscillation frequency (i.e. f-mode) of the post-merger remnant of a binary NS system. Meanwhile, using the universal relation of f mode (Krüger & Kokkotas 2020b; Manoharan et al. 2021), Völkel, Krüger & Kokkotas (2021) and Völkel & Krüger (2022) studied the Bayesian inverse problem of rotating NSs. In this work, we will study the universal relation between the f-mode frequency and the tidal deformability of SSs, which will be a useful input for comparisons among NSs, QSs, and SSs.

The paper is organized as follows. In Section 2, we introduce the EOS of SSs and obtain the structure of non-rotating SSs. Based on the background solutions, in Section 3, we integrate the equations of relativistic radial oscillations to determine the f-mode frequency for different EOSs of SSs. In Section 4, we calculate the frequency of non-radial f mode and the tidal deformability of SSs. New fits of universal relation between them are discussed. Finally, we summarize our work in Section 5.

Throughout the paper, we adopt geometric units with $c = G = 1$, where c and G denote the speed of light and the gravitational constant, respectively. The metric signature is $(-,+,+,+)$.

2 EQUATION OF STATE AND STRUCTURE OF SPHERICAL STATIC STARS

We assume that the interaction potential between two strangeons is described by the Lennard–Jones potential (Jones 1924; Lai & Xu 2009; Gao et al. 2022),

$$u(r) = 4\epsilon\left[\left(\frac{\sigma}{r}\right)^{12} - \left(\frac{\sigma}{r}\right)^{6}\right], \tag{1}$$

where ϵ is the depth of the potential, r is the distance between two strangeons, and σ is the distance when $u(r) = 0$. We note that this potential has the property of short-distance repulsion and long-distance attraction.

According to the results of early studies (Xu 2003; Lai & Xu 2009; Gao et al. 2022), the potential energy density is given by

$$\rho_{\rm p} = 2\epsilon\left(A_{12}\sigma^{12}n^{5} - A_{6}\sigma^{6}n^{3}\right), \tag{2}$$

where $A_{12} = 6.2$, $A_6 = 8.4$, and n is the number density of strangeons. The total energy density of zero-temperature dense matter composed

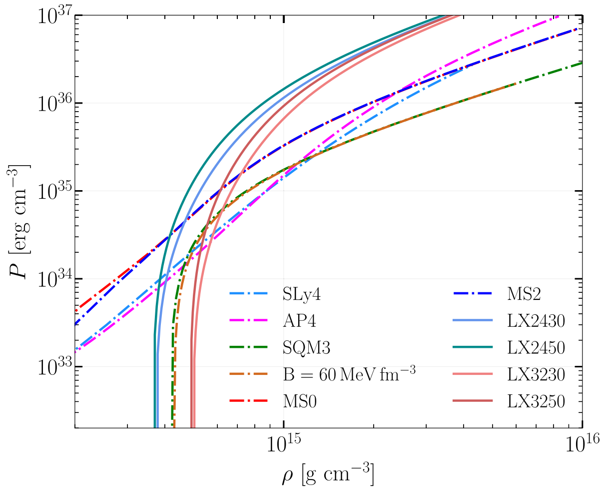

Figure 1. Relations between mass–energy density ρ and pressure P for NSs, QSs, and SSs.

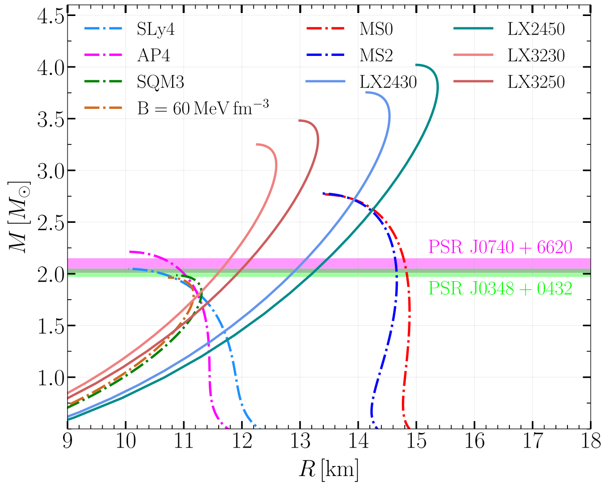

Figure 2. Mass–radius relations of SSs with different combinations of the surface baryonic density n_s and the potential depth ϵ. For comparison, we also show the mass–radius relations for selected NSs and QSs. The 1σ regions of the mass measurements in PSRs J0348+0432 (Antoniadis et al. 2013) and J0740+ 6620 (Fonseca et al. 2021) are illustrated.

of strangeons reads

$$\rho = 2\epsilon\left(A_{12}\sigma^{12}n^5 - A_6\sigma^6 n^3\right) + nN_q m_q, \tag{3}$$

where $N_q m_q$ is the mass of a strangeon with N_q being the number of quarks in a strangeon and m_q being the quark mass. In the above equation, the contributions from degenerate electrons and vibrations of the lattice are neglected. From the first law of thermodynamics, one derives the pressure

$$P = n^2\frac{\mathrm{d}(\rho/n)}{\mathrm{d}n} = 4\epsilon\left(2A_{12}\sigma^{12}n^5 - A_6\sigma^6 n^3\right). \tag{4}$$

At the surface of SSs, the pressure becomes zero and we obtain the surface number density of strangeons as $[A_6/(2A_{12}\sigma^6)]^{1/2}$. For convenience, we transform it to the number density of baryons

$$n_s = \left(\frac{A_6}{2A_{12}}\right)^{1/2}\frac{N_q}{3\sigma^3}. \tag{5}$$

For a given number of quarks N_q in a strangeon, the EOS of SSs is completely determined by the depth of the potential ϵ and the number density of baryons n_s at the surface of the star. An 18-quark cluster, called quark-alpha (Michel 1991), can be completely symmetric in spin, flavour, and colour spaces. Therefore, we set $N_q = 18$ in our calculation as a reasonable example.

Besides the EOS of SSs, we also consider six EOSs of NSs and QSs for comparison, including four popular nuclear matter EOSs for NSs, AP4 (Akmal & Pandharipande 1997), SLy4 (Douchin & Haensel 2001), MS0, and MS2 (Mueller & Serot 1996), as well as two QS models, the MIT bag model with a bag constant $B = 60\,\mathrm{MeV\,fm^{-3}}$ (Alcock et al. 1986) and SQM3 (Lattimer & Prakash 2001).[1] The corresponding density–pressure relations for these EOSs are depicted in Fig. 1. We denote the EOSs of SSs using their values of n_s and ϵ. For example, 'LX2430' means a surface baryon number density $n_s = 0.24\,\mathrm{fm^{-3}}$ and a potential depth $\epsilon = 30\,\mathrm{MeV}$.

We consider the unperturbed relativistic star to be described by a perfect fluid. The energy–momentum tensor is $T_{\mu\nu} = (\rho + P)u_\mu u_\nu + P\,g_{\mu\nu}$. The static and spherically symmetric metric, which describes an equilibrium relativistic star, is given by the line element,

$$\mathrm{d}s^2 = -e^{2\Phi}\mathrm{d}t^2 + e^{2\Lambda}\mathrm{d}r^2 + r^2(\mathrm{d}\theta^2 + \sin^2\theta\,\mathrm{d}\phi^2), \tag{6}$$

where Φ and Λ are metric functions of r. A mass function $m(r)$ is defined as $m(r) = r(1 - e^{-2\Lambda})/2$, which satisfies

$$\frac{\mathrm{d}m}{\mathrm{d}r} = 4\pi r^2\rho, \tag{7}$$

where ρ is the energy density. The Tolman–Oppenheimer–Volkoff equations that determine the pressure $P(r)$ and the metric function $\Phi(r)$ are expressed as

$$\frac{\mathrm{d}P}{\mathrm{d}r} = -(\rho + P)\frac{\mathrm{d}\Phi}{\mathrm{d}r}, \tag{8}$$

$$\frac{\mathrm{d}\Phi}{\mathrm{d}r} = \frac{m + 4\pi r^3 P}{r(r - 2m)}. \tag{9}$$

Integrating equations (7), (8), and (9) combined with the EOS, one obtains the stellar structure of spherical stars and the space–time geometry. In Fig. 2, we show the mass–radius relations for NSs, QSs, and SSs using the aforementioned EOSs. The EOSs of SSs are very stiff because the strangeons are non-relativistic and there is a very strong repulsion at a short intercluster distance (Gao et al. 2022), which leads to the maximal masses over $3\,\mathrm{M_\odot}$. In contrast, the quarks are relativistic and nearly free for QSs, so the EOSs are soft and the maximal masses only reach $2\,\mathrm{M_\odot}$ marginally. The observations of the massive pulsars, PSRs J0348+0432 (Antoniadis et al. 2013) and J0740+6620 (Fonseca et al. 2021), at $\sim 2\,\mathrm{M_\odot}$ via pulsar timing support the stiff properties of the EOS. More massive ones (e.g. $\geq 2.5\,\mathrm{M_\odot}$) are expected in our model for future discovery. The GWs from the binary NS inspiral, GW170817, gave constraints on the tidal deformability for the first time (Abbott et al. 2017, 2018, 2019a), which rules out several stiff EOSs (e.g. EOSs MS0 and MS2) and models of SSs with very low surface baryonic densities (say, LX2430 and LX2450) at a 90 per cent credible level (see fig. 18 in Gao et al. 2022).

[1] Note that the nucleonic EOSs, MS0, and MS2 have similar properties as SSs of higher maximum masses.

3 RADIAL OSCILLATIONS

In this section, we study radial oscillations of SSs. We denote the radial displacement of a fluid element as $\delta r(r, t)$ and its harmonic oscillation mode with circular frequency ω as $\delta r(r, t) = X(r)e^{i\omega t}$. To obtain the discrete set of oscillation frequencies of SSs, we adopt the perturbation equations in Kokkotas & Ruoff (2001). In practice, we define a new variable $\zeta = r^2 e^{-\Phi} X$. The master equation for radial oscillations is expressed as

$$\frac{\mathrm{d}}{\mathrm{d}r}\left(\mathcal{P}\frac{\mathrm{d}\zeta}{\mathrm{d}r}\right) + \left(\mathcal{Q} + \omega^2 \mathcal{W}\right)\zeta = 0, \tag{10}$$

where

$$\begin{aligned} r^2\mathcal{P} &= \Gamma P\, e^{(\Lambda+3\Phi)}, \\ r^2\mathcal{Q} &= e^{(\Lambda+3\Phi)}(\rho + P)\left[(\Phi')^2 + 4\frac{\Phi'}{r} - 8\pi e^{2\Lambda} P\right], \\ r^2\mathcal{W} &= (\rho + P)e^{(3\Lambda+\Phi)}. \end{aligned} \tag{11}$$

By setting $\eta = \mathcal{P}\zeta'$, one obtains the following coupled differential equations,

$$\frac{\mathrm{d}\zeta}{\mathrm{d}r} = \frac{\eta}{\mathcal{P}}, \tag{12}$$

$$\frac{\mathrm{d}\eta}{\mathrm{d}r} = -\left(\omega^2\mathcal{W} + \mathcal{Q}\right)\zeta. \tag{13}$$

At the centre of the star, the boundary condition is $3\zeta_0 = \eta_0/\mathcal{P}_0$, where ζ_0 and η_0 are the values of ζ and η at $r = 0$, respectively (Kokkotas & Ruoff 2001). By setting $\eta_0 = 1$, we have $\zeta_0 = 1/3\mathcal{P}_0$, where $\mathcal{P}_0 = \Gamma P(0)e^{(\Lambda(0)+3\Phi(0))}$. At the star surface $r = R$, the pressure perturbation must vanish, namely $\Delta P = 0$, which provides another boundary condition, $\Gamma P\zeta' = 0$. Equations (12) and (13) with the above two boundary conditions form a two-point boundary value problem of the Sturm–Liouville type with eigenvalues $\omega_0^2 < \omega_1^2 < \omega_2^2 < \cdots$ (Shapiro & Teukolsky 1983), where ω_0 is the eigenfrequency of the f mode. If $\omega_0^2 > 0$, all the eigenfrequencies of the oscillation modes are real, which indicates that the equilibrium stellar model is dynamically stable (Chandrasekhar 1964a,b; Misner et al. 1973). The period of the f mode is given by $\tau_0 = 1/\nu_0 = 2\pi/\omega_0$, where ν_0 is the ordinary or temporal frequency. Inversely, $\omega_0^2 < 0$ corresponds to an exponentially growing unstable radial oscillation.

For adiabatic oscillations, the adiabatic index governing the perturbations is defined by (Kokkotas & Ruoff 2001)

$$\Gamma = \frac{\rho + P}{P}\frac{\mathrm{d}P}{\mathrm{d}\rho}, \tag{14}$$

which is equal to the adiabatic index governing the equilibrium pressure–energy density relation. The relation between the adiabatic index Γ and the mass–energy density ρ is shown in Fig. 3. We note that the adiabatic indices for QSs and SSs are qualitatively different from that of NSs at low density. Moreover, SSs generally have a larger adiabatic index than NSs and QSs, indicating that the EOSs of SSs are stiffer (Gao et al. 2022).

In Fig. 4, we present the f-mode frequency ν_0 and the frequencies of the first two excited modes, ν_1 and ν_2, for SLy4, AP4, and the MIT bag model. Our results for NSs reproduce the results of Kokkotas & Ruoff (2001). We observe that f mode becomes unstable (i.e. ω_0^2 becoming negative) for central densities above 2.83×10^{15}, 2.70×10^{15}, and $2.05 \times 10^{15}\,\mathrm{g\,cm^{-3}}$ for three EOSs. The instability point corresponds to maximal masses 2.04, 2.21, and 1.96 $\mathrm{M_\odot}$ for SLy4, AP4, and the MIT bag model, respectively. It is worth noting that the f-mode frequency of the MIT bag model behaves very different from that of NSs at low central density, rooting in the self-bound and gravity-bound nature of QSs and NSs, respectively.

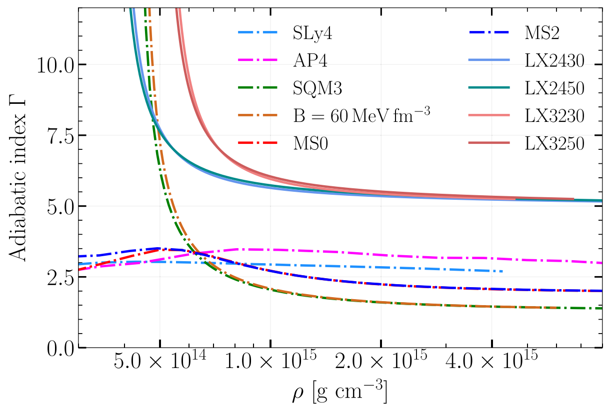

Figure 3. Relation between the adiabatic index Γ and the mass–energy density ρ for NSs, QSs, and SSs.

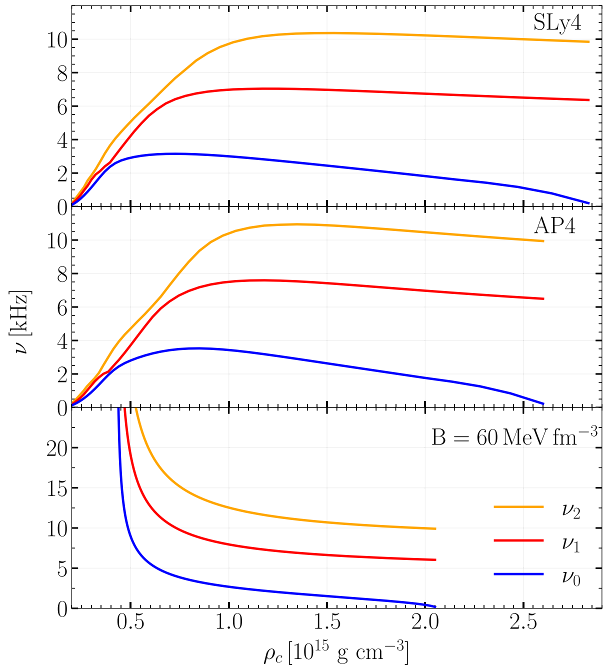

Figure 4. The frequencies of the fundamental mode, ν_0, and the first two excited modes, ν_1 and ν_2, of radial oscillation, as functions of the central density ρ_c for NSs and QSs.

To further explore the results for QSs, SSs, and NSs, we note that with a low central density, the star can be approximated as a homogeneous non-relativistic star (Shapiro & Teukolsky 1983), so that the angular frequency ω_0 of the f mode reads $\omega_0^2 = 4\pi\rho(4\Gamma - 3)/3$. Using the relations between the density and the adiabatic index shown in Fig. 3, we do expect the frequency ω_0 to diverge as the density approaches a minimal value for QSs and SSs. For NSs, the adiabatic index does not change significantly as the density decreases. Therefore for NSs, ω_0 tends to zero mildly when the central density of the star is sufficiently low. Indeed, these points are confirmed in Fig. 4.

In Fig. 5, we show the ordinary frequency ν_0 of the f mode versus the mass of the stars for SSs and one EOS of QSs. The curves of SSs have the same trend as that of QSs, with ν_0 going to zero at their maximal masses. However, ν_0 for SSs is larger than that of QSs for

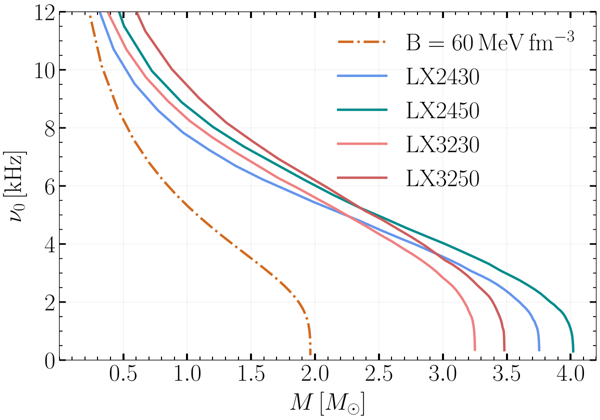

Figure 5. The frequencies of the fundamental mode ν_0 as functions of the mass M for QSs and SSs.

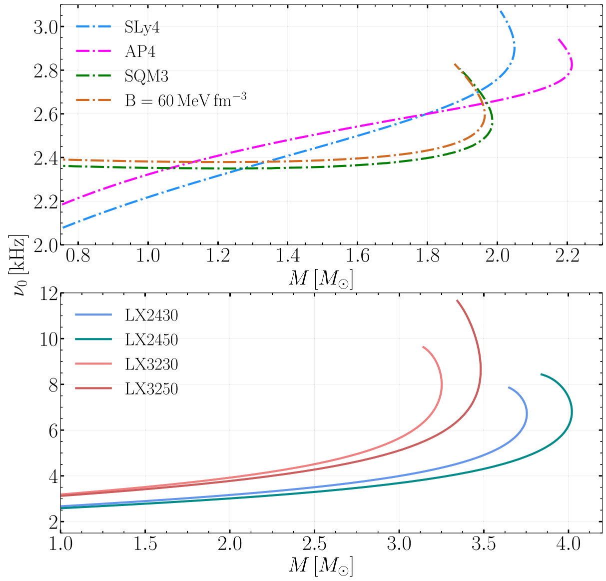

Figure 6. The frequency ν_0 of f mode as a function of mass M for NSs and QSs (top) and SSs (bottom).

a given mass, which arises from the fact that SSs' EOSs are much stiffer than that of QSs.

4 NON-RADIAL OSCILLATIONS

In this section, we study non-radial oscillations of a non-rotating SS in the Cowling approximation, in which the space–time metric is kept to be the static spherical background solution in the so-called Cowling approximation (Cowling 1941). The fluid Lagrangian displacement vector is given by

$$\xi^i = \left(e^{-\Lambda} W, -V\partial_\theta, -V\sin^{-2}\theta\partial_\phi\right) r^{-2} Y_{\ell m}, \tag{15}$$

where W and V are functions of t and r, while $Y_{\ell m}$ is the spherical harmonic function. Then the perturbation of the four-velocity, δu^μ, can be written as

$$\delta u^\mu = \left(0, e^{-\Lambda}\partial_t W, -\partial_t V\partial_\theta, -\partial_t V\sin^{-2}\theta\partial_\phi\right) r^{-2} e^{-\Phi} Y_{\ell m}. \tag{16}$$

Assuming a harmonic dependence on time, the perturbative variables can be written as $W(t, r) = W(r)e^{i\omega t}$ and $V(t, r) = V(r)e^{i\omega t}$. We can obtain the following system of equations for the fluid perturbations (see Sotani et al. 2011; Doneva & Yazadjiev 2012; Yazadjiev & Doneva 2012, for a detailed variational derivation),

$$\frac{\mathrm{d}W}{\mathrm{d}r} = \frac{\mathrm{d}\rho}{\mathrm{d}P}\left[\omega^2 r^2 e^{\Lambda-2\Phi} V + \frac{\mathrm{d}\Phi}{\mathrm{d}r} W\right] - \ell(\ell+1)e^{\Lambda} V, \tag{17}$$

$$\frac{\mathrm{d}V}{\mathrm{d}r} = 2\frac{\mathrm{d}\Phi}{\mathrm{d}r} V - e^{\Lambda}\frac{W}{r^2}. \tag{18}$$

The boundary condition at the centre of the star can be parametrized as, $W = Ar^{l+1}$ and $V = -Ar^l/l$, with A being an arbitrary constant. It can be obtained by examining the behaviour of W and V in the vicinity of $r = 0$. At the surface of the star, the perturbed pressure must vanish, which provides

$$\omega^2 e^{\Lambda(R)-2\Phi(R)} V(R) + \frac{1}{R^2}\frac{\mathrm{d}\Phi}{\mathrm{d}r}\bigg|_{r=R} W(R) = 0. \tag{19}$$

In full general relativity, each QNM is characterized by a complex eigenfrequency $\omega = \omega_{\mathrm{r}} + \mathrm{i}\,\omega_{\mathrm{i}}$ (Thorne & Campolattaro 1967). The real part ω_{r} corresponds to the mode frequency, and the imaginary part ω_{i} gives the damping time $\tau \equiv 1/\omega_{\mathrm{i}}$ due to GW emission. However, in the Cowling approximation, we obtain normal modes of oscillation and there is no emission of GWs. For a non-rotating stellar model, the Cowling approximation leads to a relative error $\sim$ 10–30 per cent for the f mode (Chirenti, de Souza & Kastaun 2015; Sotani & Dohi 2022). For higher modes, the relative error is smaller (Yoshida & Kojima 1997).

4.1 F-mode frequency

Now we calculate the ordinary frequency ν_0 of the f mode for the $l = 2$ non-radial oscillation, and study its relation with the mass M, the compactness $C = M/R$, and the dimensionless tidal deformability Λ for NSs, QSs, and SSs.

The frequency ν_0 versus mass M for NSs and QSs is shown in the top panel of Fig. 6. By increasing the mass of the star, the frequency ν_0 increases significantly for NSs, while it does not change much for QSs. This can be understood by noticing that QSs are self-bound by strong interaction and the density in the interior of the star does not change too much as the mass increases. This is in contrast to NSs that are gravitationally bound. From the figure, we can see that the values of ν_0 at the maximal masses of NSs and QSs are 2.907, 2.823, 2.562, and 2.597 kHz for SLy4, AP4, SQM3, and the MIT bag model with $B = 60\,\mathrm{MeV\,fm^{-3}}$, respectively.

Additionally, the frequency ν_0 versus mass M for SSs is shown in the bottom panel of Fig. 6. We find that the curves of SSs are similar to those of QSs only that the frequency ν_0 for SSs extends a much wider range. The values of ν_0 at the maximal masses of SSs are 6.676, 6.832, 7.977, and 8.684 kHz for the EOSs of SSs with different values of n_{s} and ϵ that we use in the figure. Compared with QSs and NSs, these values are much larger, and it could be an indicator to distinguish EOSs via GW observations.

We show in Fig. 7 the relation between the frequency ν_0 and the compactness of the stars. It might be useful to note that the values of the maximal compactness, $C_{\max}$, are 0.21, 0.23, 0.19, and 0.19 for SLy4, AP4, SQM3, and the MIT bag model with $B = 60\,\mathrm{MeV\,fm^{-3}}$, respectively. In contrast, the value of $C_{\max}$ for SSs with different values of n_{s} and ϵ is about the same, $C_{\max} \simeq 0.27$. This maximal value of the compactness represents the limit of how stiff EOSs of SSs can be due to the repulsive hardcore and the non-relativistic nature of strangeons.

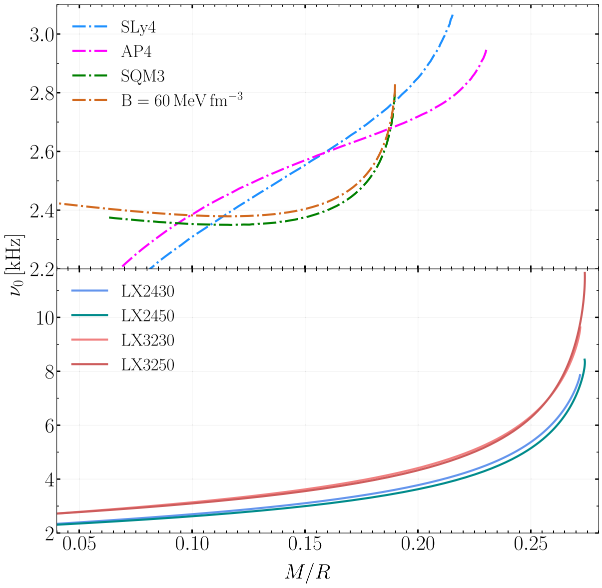

Figure 7. The frequency ν_0 of the f mode as a function of the compactness, $C = M/R$, for NSs and QSs (top) and SSs (bottom).

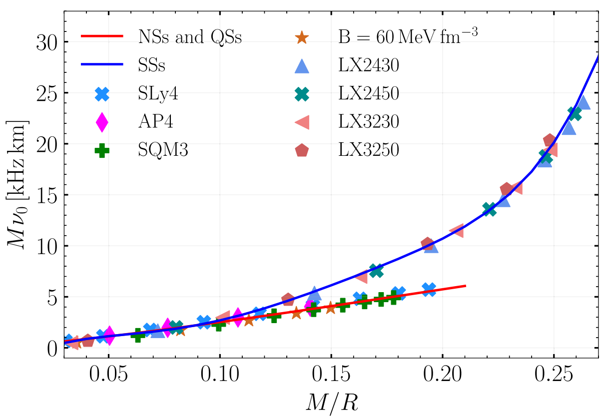

Figure 8. Scaled frequency of the f mode as a function of the compactness C. The solid lines represent universal relations in equations (20) and (21).

4.2 Universal relations

To reveal the internal characters of NSs and assist relevant data analysis, universal relations between the f-mode, p-mode, and w-mode frequencies and the mass or the radius of NSs have been investigated (Andersson & Kokkotas 1996, 1998; Benhar, Berti & Ferrari 1999; Benhar et al. 2004; Tsui & Leung 2005). Motivated by possible observations of the moment of inertia I of NSs, Lau, Leung & Lin (2010) used the moment of inertia to replace the compactness and discovered EOS-independent relations in QNMs of NSs and QSs. Similar results were shown in Chirenti et al. (2015). These relations can be used to infer the stellar parameters – mass, radius, and possibly the EOS – from QNM data with future GW detectors.

Using the Cowling approximation, Sotani et al. (2011) calculated non-radial oscillations of NSs with hadron–quark mixed phase transition, and discovered an approximate formula. Inspired by the universal relation between the f mode and the compactness C (Sotani et al. 2011), we show the scaled frequency of the f mode versus the compactness C for NSs, QSs, and SSs in Fig. 8. In

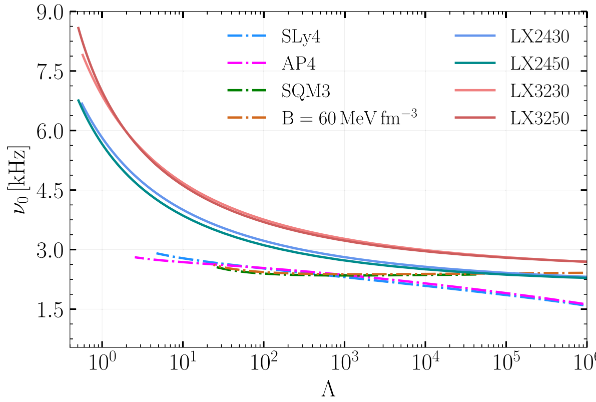

Figure 9. The frequency of the f mode as a function of the dimensionless tidal deformability Λ for NSs, QSs, and SSs.

particular, as shown by the solid lines in the figure, the universal relation for NSs can be represented by the following empirical formula:

$$M\nu_0 = a_{\rm I} + b_{\rm I}\left(\frac{M}{R}\right) + c_{\rm I}\left(\frac{M}{R}\right)^2 + d_{\rm I}\left(\frac{M}{R}\right)^3, \tag{20}$$

with $a_{\rm I} = -0.012$, $b_{\rm I} = 19.48$, $c_{\rm I} = 71.3$, and $d_{\rm I} = -125$, while for SSs, we found a new universal relation,

$$M\nu_0 = a_{\rm II} + b_{\rm II}\left(\frac{M}{R}\right) + c_{\rm II}\left(\frac{M}{R}\right)^2 + d_{\rm II}\left(\frac{M}{R}\right)^3 + e_{\rm II}\left(\frac{M}{R}\right)^4 + k_{\rm II}\left(\frac{M}{R}\right)^5, \tag{21}$$

with $a_{\rm II} = -2.795$, $b_{\rm II} = 1.941 \times 10^2$, $c_{\rm II} = -3.834 \times 10^3$, $d_{\rm II} = 3.789 \times 10^4$, $e_{\rm II} = -1.601 \times 10^5$, and $k_{\rm II} = 2.531 \times 10^5$. We can observe that the behaviour of the f-mode frequencies for the SSs is very different from the NSs and QSs, especially when the compactness is larger than $\sim$0.15, where the f-mode frequency from SSs is much larger than that of QSs and NSs. It can be an important 'smoking gun' signal for SSs.

For tidally deformed relativistic stars, the quadrupole tidal deformability gives important information about the stellar structure. To characterize the deformation of the star, one usually defines the tidal deformability via $Q_{ij} \equiv -\lambda\mathcal{E}_{ij}$, where $\mathcal{E}_{ij}$ is the external tidal field and Q_{ij} is the induced traceless quadrupole moment tensor of stars (Hinderer 2008; Hinderer et al. 2010). The parameter λ is related to the $l = 2$ Love number k_2 via $k_2 = 3\lambda R^{-5}/2$. Besides, the dimensionless tidal deformability Λ, defined as $\Lambda = 2k_2C^{-5}/3$, is also commonly used. We note that the tidal deformability is proportional to the fifth power of the radius R. Therefore, constraining or measuring tidal deformability can provide important information on the EOS (Abbott et al. 2018, 2019a), as well as test gravity theories (Hu et al. 2021; Xu, Gao & Shao 2022). The influence of tidal on the phase of GW in the inspiral stage is predominantly dependent on the Love number k_2, and the effect enters at the fifth post-Newtonian (PN) order (Flanagan & Hinderer 2008).

In Fig. 9, we display the relation between the frequency of the f mode and the dimensionless tidal deformability, Λ, for NSs, QSs, and SSs. It is seen that the frequency decreases with Λ. It is understood that the more compact the star becomes the harder it can be deformed. For SSs, as the potential depth ϵ increases and the surface baryonic density $n_{\rm s}$ decreases, the EOS becomes stiffer, which leads to larger tidal deformability and f-mode frequency.

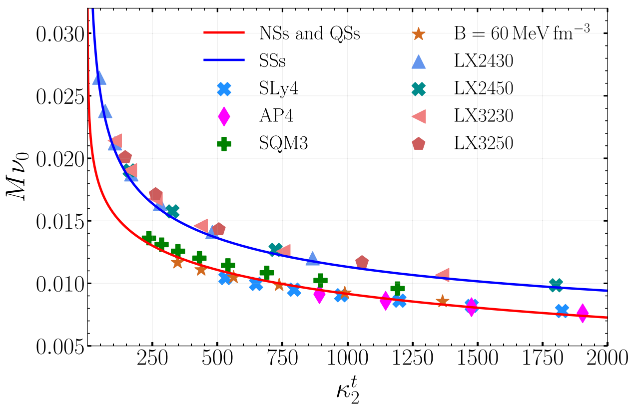

Figure 10. Scaled frequency of the f-mode $M\nu_0$ as a function of the tidal quadrupolar ($l = 2$) coupling constant κ_2^t for NSs, QSs, and SSs. The solid line represents the best power-law fit in κ_2^t to the scaled frequencies of the NSs, QSs, and SSs.

For binary NSs of masses M_a and M_b, the dimensionless tidal coupling constant is defined as (Bernuzzi et al. 2014, 2015a,b)

$$\kappa_2^t = 2\left[q\left(\frac{X_a}{C_a}\right)^5 k_2^a + \frac{1}{q}\left(\frac{X_b}{C_b}\right)^5 k_2^b\right], \tag{22}$$

where $q = M_b/M_a \le 1$, $X_a = M_a/(M_a + M_b)$, and C_i and k_2^i ($i = a, b$) are the compactness and the quadrupole Love number of each star. If we consider a binary system with non-rotating equal-mass configuration, the dimensionless tidal coupling constant is given by $\kappa_2^t = k_2/8C^5 = 3\Lambda/16$.

Inspired by the universal relation between the dimensionless tidal coupling constant and the f-mode frequency (Chakravarti & Andersson 2020), the relation between $M\nu_0$ and κ_2^t for NSs, QSs, and SSs are shown in Fig. 10. For NSs and QSs, we find the scaled frequency of the f mode approximately satisfies the following relation,

$$M\nu_0 = 0.184(\kappa_2^t)^{-0.016} - 0.154. \tag{23}$$

For SSs, the universal relation is

$$M\nu_0 = 0.071(\kappa_2^t)^{-0.266}. \tag{24}$$

The universal relations for QSs and SSs will complement that of NSs, and play a role in GW data analysis (Dietrich, Bernuzzi & Tichy 2017).

5 CONCLUSIONS

In this paper, we use the Lennard–Jones model to describe the EOS of SSs with two parameters, the number density at the surface of the star n_s and the potential depth ϵ. Compared to the MIT bag model of QSs, the EOS of SSs is much stiff due to the non-relativistic nature of the particles and the compressed repulsive hardcore at a small intercluster distance. Following earlier work (Lai & Xu 2009; Gao et al. 2022), we calculate the mass and radius relation for SSs for different values of n_s and ϵ, and find that the maximal mass of SSs is higher than that of NSs and QSs. This serves as background solutions for perturbation studies of various oscillation modes.

To study radial oscillations of SSs, for the first time we calculate the frequency of the radial modes for SSs with different combinations of n_s and ϵ. The results are compared with that of NSs and QSs. We discover that radial oscillations of SSs are similar to those of QSs but behave very differently from those of NSs, especially for stars with low central energy densities or small masses. For QSs and SSs, the frequencies of radial oscillations tend to infinity when the central energy density approaches the minimal value $\rho_{\rm min}$, which corresponds to the pressure being zero. This can be understood by approximating the stars in the non-relativistic regime and noticing that the adiabatic index Γ for SSs and QSs goes to infinity as the density decreases to its minimal value.

For non-radial oscillations of SSs, we calculate the frequency of the f mode for $l = 2$ component using the Cowling approximation, and obtain the universal relations between the f-mode frequency and other global parameters of the spherical SSs. As recently proposed in Gao et al. (2022), where the I–Love–Q universal relations for SSs were studied, the universal relation of the f-mode frequency for SSs is also ready to be used for various purposes in GW astrophysics involving compact stars. With application to data in the future, possible constraints can be set on the parameter space of the Lennard–Jones model, namely the n_s–ϵ plane, using GW observations of the QNMs from compact stars.

There can be several interesting extensions of our work. First, our study of non-radial oscillations uses the Cowling approximation (Cowling 1941), which considers only the fluid perturbation. In principle, one should also allow the space–time metric to be perturbed, and thus one can obtain QNMs instead of normal modes. Next, we would like to further investigate how dynamical tides affect the frequency of the f mode in compact binary systems. NSs have certain spins and the rotation rate may reach extreme values, especially for nascent or remnant objects following a binary merger. From the perspective of detecting oscillation modes with GWs, the most relevant scenarios are likely to involve rapidly rotating NSs. An important step in this direction has been carried out using perturbation theory in general relativity with the Cowling approximation (Krüger, Gaertig & Kokkotas 2010; Gaertig & Kokkotas 2011; Doneva et al. 2013). In the next step, we can study the oscillation modes of rapidly rotating SSs in the Cowling approximation based on existing work. Recently, Krüger & Kokkotas (2020a,b), managed to calculate the oscillations and instabilities of relativistic stars using perturbation theory without the Cowling approximation. The oscillation spectrum, universal relations involving f mode, and the critical values for the onset of the secular Chandrasekhar–Friedman–Schutz instability are studied in great detail. Further, Manoharan et al. (2021) investigated universal relations for binary NS mergers with long-lived remnants. By considering the oscillations of the rapidly rotating merger remnant, they proposed an approach to relate the pre-merger tidal deformability to the effective compactness of the post-merger remnant. Those studies are important to probe the EOS of NSs with GW asteroseismology. Therefore, to study the oscillations of rapidly rotating SSs without the Cowling approximation is an important goal worth pursuing.

ACKNOWLEDGEMENTS

We thank Christian Krüger for useful comments. This work was supported by the National SKA Program of China (2020SKA0120300, 2020SKA0120100), the National Natural Science Foundation of China (11975027, 11991053, 11721303), the National Key R&D Program of China (2017YFA0402602), the Max Planck Partner Group Program funded by the Max Planck Society, and the High-Performance Computing Platform of Peking University. RX was supported by the Boya Postdoctoral Fellowship at Peking University.

DATA AVAILABILITY

The data underlying this paper will be shared on reasonable request to the corresponding authors.

REFERENCES

Abbott B. P. et al., 2017, Phys. Rev. Lett., 119, 161101
Abbott B. P. et al., 2018, Phys. Rev. Lett., 121, 161101
Abbott B. P. et al., 2019a, Phys. Rev. X, 9, 011001
Abbott B. P. et al., 2019b, Phys. Rev. Lett., 122, 061104
Abbott R. et al., 2022, Prog. Theor. Exp. Phys., 2022, 063F01
Abe H. et al., 2022, Galaxies, 10, 63
Akmal A., Pandharipande V. R., 1997, Phys. Rev. C, 56, 2261
Alcock C., Farhi E., Olinto A., 1986, ApJ, 310, 261
Alford M. G., Schmitt A., Rajagopal K., Schäfer T., 2008, MNRAS, 80, 1455
Allen G., Andersson N., Kokkotas K. D., Schutz B. F., 1998, Phys. Rev. D, 58, 124012
Andersson N., 2019, Gravitational-Wave Astronomy: Exploring the Dark Side of the Universe. Oxford Univ. Press, Oxford
Andersson N., Kokkotas K. D., 1996, Phys. Rev. Lett., 77, 4134
Andersson N., Kokkotas K. D., 1998, MNRAS, 299, 1059
Antoniadis J. et al., 2013, Science, 340, 6131
Benhar O., Berti E., Ferrari V., 1999, MNRAS, 310, 797
Benhar O., Ferrari V., Gualtieri L., 2004, Phys. Rev. D, 70, 124015
Bernuzzi S., Nagar A., Balmelli S., Dietrich T., Ujevic M., 2014, Phys. Rev. Lett., 112, 201101
Bernuzzi S., Nagar A., Dietrich T., Damour T., 2015a, Phys. Rev. Lett., 114, 161103
Bernuzzi S., Dietrich T., Nagar A., 2015b, Phys. Rev. Lett., 115, 091101
Chakravarti K., Andersson N., 2020, MNRAS, 497, 5480
Chan T. K., Sham Y. H., Leung P. T., Lin L. M., 2014, Phys. Rev. D, 90, 124023
Chandrasekhar S., 1964a, Phys. Rev. Lett., 12, 114
Chandrasekhar S., 1964b, ApJ, 140, 417
Chandrasekhar S., Ferrari V., 1991, Proc. R. Soc. A, 432, 247
Chirenti C., de Souza G. H., Kastaun W., 2015, Phys. Rev. D, 91, 044034
Cowling T. G., 1941, MNRAS, 101, 367
Das H. C., Kumar A., Biswal S. K., Patra S. K., 2021, Phys. Rev. D, 104, 123006
Demorest P., Pennucci T., Ransom S., Roberts M., Hessels J., 2010, Nature, 467, 1081
Detweiler S. L., Lindblom L., 1985, ApJ, 292, 12
Dietrich T., Bernuzzi S., Tichy W., 2017, Phys. Rev. D, 96, 121501
Doneva D. D., Yazadjiev S. S., 2012, Phys. Rev. D, 85, 124023
Doneva D. D., Gaertig E., Kokkotas K. D., Krüger C., 2013, Phys. Rev. D, 88, 044052
Douchin F., Haensel P., 2001, A&A, 380, 151
Flanagan E. E., Hinderer T., 2008, Phys. Rev. D, 77, 021502
Fonseca E. et al., 2021, ApJL, 915, L12
Gaertig E., Kokkotas K. D., 2011, Phys. Rev. D, 83, 064031
Gao Y., Lai X. Y., Shao L., Xu R. X., 2022, MNRAS, 509, 2758
Glass E. N., Lindblom L., 1983, ApJS, 53, 93
Gondek D., Haensel P., Zdunik J. L., 1997, A&A, 325, 217
Hinderer T., 2008, ApJ, 677, 1216
Hinderer T., Lackey B. D., Lang R. N., Read J. S., 2010, Phys. Rev. D, 81, 123016
Hu Z., Gao Y., Xu R., Shao L., 2021, Phys. Rev. D, 104, 104014
Jones J. E., 1924, Proc. R. Soc. A, 106, 463
Kalogera V. et al., 2021, preprint (arXiv:2111.06990)
Kasen D., Metzger B., Barnes J., Quataert E., Ramirez-Ruiz E., 2017, Nature, 551, 80
Kasliwal M. M. et al., 2017, Science, 358, 1559
Kiuchi K., Kawaguchi K., Kyutoku K., Sekiguchi Y., Shibata M., 2020, Phys. Rev. D, 101, 084006
Kokkotas K. D., Ruoff J., 2001, A&A, 366, 565
Kokkotas K. D., Schmidt B. G., 1999, Living Rev. Relativ., 2, 2
Kokkotas K. D., Schutz B. F., 1992, MNRAS, 255, 119
Krüger C. J., Kokkotas K. D., 2020a, Phys. Rev. D, 102, 064026
Krüger C. J., Kokkotas K. D., 2020b, Phys. Rev. Lett., 125, 111106
Krüger C. J., Gaertig E., Kokkotas K. D., 2010, Phys. Rev. D, 81, 084019
Lai X. Y., Xu R. X., 2009, MNRAS, 398, 31
Lai X. Y., Xu R. X., 2017, J. Phys. Conf. Ser., 861, 012027
Lai X. Y., Yu Y. W., Zhou E. P., Li Y. Y., Xu R. X., 2018a, Res. Astron. Astrophys., 18, 024
Lai X. Y., Yun C. A., Lu J. G., Lü G. L., Wang Z. J., Xu R. X., 2018b, MNRAS, 476, 3303
Lai X. Y., Zhou E. P., Xu R. X., 2019, Eur. Phys. J. A, 55, 60
Lai X. Y., Xia C. J., Yu Y. W., Xu R. X., 2021, Res. Astron. Astrophys., 21, 250
Lattimer J. M., Prakash M., 2001, ApJ, 550, 426
Lattimer J. M., Prakash M., 2007, Phys. Rep., 442, 109
Lau H. K., Leung P. T., Lin L. M., 2010, ApJ, 714, 1234
Lindblom L., Detweiler S. L., 1983, ApJS, 53, 73
Lu J. et al., 2019, Sci. China Phys. Mech. Astron., 62, 959505
Manoharan P., Krüger C. J., Kokkotas K. D., 2021, Phys. Rev. D, 104, 023005
Michel F. C., 1991, Nucl. Phys. B Proc. Suppl., 24, 33
Misner C. W., Thorne K. S., Wheeler J. A., 1973, Gravitation. W. H. Freeman, San Francisco, p. 688
Mueller H., Serot B. D., 1996, Nucl. Phys. A, 606, 508
Ozel F., Baym G., Guver T., 2010, Phys. Rev. D, 82, 101301
Peng C., Xu R. X., 2008, MNRAS, 384, 1034
Punturo M. et al., 2010, Class. Quantum Gravity, 27, 194002
Rezzolla L., Takami K., 2016, Phys. Rev. D, 93, 124051
Sathyaprakash B. S. et al., 2019, Bull. Am. Astron. Soc., 51, 251
Shapiro S. L., Teukolsky S. A., 1983 Black Holes, White Dwarfs, and Neutron Stars: The Physics of Compact Objects. Wiley-VCH, New York, p. 127
Sotani H., Dohi A., 2022, Phys. Rev. D, 105, 023007
Sotani H., Kumar B., 2021, Phys. Rev. D, 104, 123002
Sotani H., Yasutake N., Maruyama T., Tatsumi T., 2011, Phys. Rev. D, 83, 024014
Thorne K. S., Campolattaro A., 1967, ApJ, 149, 591
Tsui L. K., Leung P. T., 2005, MNRAS, 357, 1029
Vaeth H. M., Chanmugam G., 1992, A&A, 260, 250
Völkel S. H., Krüger C. J., 2022, Phys. Rev. D, 105, 124071
Völkel S. H., Krüger C. J., Kokkotas K. D., 2021, Phys. Rev. D, 103, 083008
Wang W. H., Lai X. Y., Zhou E. P., Lu J. G., Zheng X. P., Xu R. X., 2020, MNRAS, 500, 5336
Witten E., 1984, Phys. Rev. D, 30, 272
Xu R. X., 2003, ApJ, 596, L59
Xu R. X., Guo Y. J., 2017, in Vasconcellos C. A. Z., ed., 11th Rencontres du Vietnam: Hot Topics in General Relativity and Gravitation. World Scientific Publishing Co. Pte. Ltd., London, p. 119
Xu R. X., Qiao G. J., Zhang B., 1999, ApJL, 522, L109
Xu R. X., Gao Y., Shao L., 2022, Phys. Rev. D, 105, 024003
Yagi K., Yunes N., 2013a, Phys. Rev. D, 88, 023009
Yagi K., Yunes N., 2013b, Science, 341, 365
Yazadjiev S. S., Doneva D. D., 2012, J. Cosmol. Astropart. Phys., 03, 037
Yoshida S., Kojima Y., 1997, MNRAS, 289, 117
Zhou A. Z., Xu R. X., Wu X. J., Wang N., 2004, Astropart. Phys., 22, 73
Zhou E. P., Lu J. G., Tong H., Xu R. X., 2014, MNRAS, 443, 2705

This paper has been typeset from a TEX/LATEX file prepared by the author.